Supporting Information

Versatile phosphate diester based flame retardant vitrimers via catalyst-free mixed transesterification

Xiaming Feng, Guoqiang Li*

Department of Mechanical & Industrial Engineering, Louisiana State University, Baton Rouge, LA 70803, United States

**Corresponding author. E-mail: lguoqi1@lsu.edu; Tel.: 001-225-578-5302*

Calculations.

Calculation of the cross-linking density (δ) can be performed using Eqs. (1)[1-2]:

$$\delta = E' / 3RT \qquad (1)$$

where R is universal gas constant (8.314 $m^3 \cdot Pa/K \cdot mol$); T is absolute temperature (455.55 K), and E' is storage modulus (75.7 MPa) at rubber state (T_g + 30 °C). The δ value for the BPA network at T_g + 30 °C is found to be 7.1×10^3 mol/m^3.

For determining activation energy (E_a) of the BPA network. The relaxation time τ were fitted to the Arrhenius equation (Eq. (2)):

$$\ln \tau(t) = \ln \tau_0 + E_a / RT \qquad (2)$$

where R is universal gas constant (8.314 $m^3 \cdot Pa/K \cdot mol$); T is absolute temperature; the characteristic relaxation time τ can be obtained from the stress relaxation test at elevated temperatures. E_a is the activation energy of the BPA networks determined by Figure 2b.

T_v is defined as the liquid-to-solid transition temperature, where the viscosity (η) is 10^{12} Pa·s. The T_v value was obtained using Maxwell's relation (Eq. (3)) and Arrhenius relationship (Eq. (2))[1-2].

$$\eta = \tau E' / 2(1 + \nu) \qquad (3)$$

where ν is Poisson's ratio (0.3); E' is storage modulus (75.7 MPa) at stable rubbery state (T_g + 30 °C); By inputting the values of Poisson's ratio and E' and $\eta = 10^{12}$ Pa·s into equation (3), an extrapolated relaxation time τ = 34,346 s is obtained. By plugging this extrapolated relaxation time back into the linear fitting equation (4) (Figure 2c) of equation (2), the calculated T_v is about 9.1 °C.

$$y = 5.15\,x - 7.80 \qquad (4)$$

where x is 1000/T (K^{-1}) and y is ln τ (s).

Figure S1. Photos of the HDA monomer with 3 wt% photo initiator (upper left) and its UV cured polymer (upper right), the BPA monomer with 3 wt% photo initiator (lower left) and its UV cured polymer (lower right).

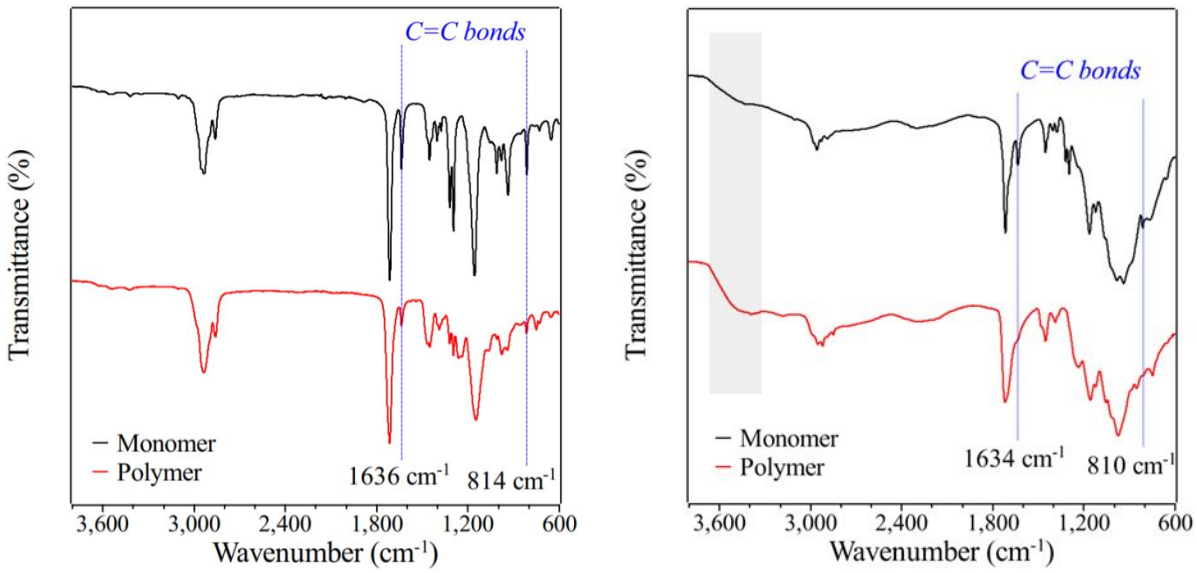

Figure S2. FTIR of the HDA monomer and its UV cured polymer (left). FTIR of the BPA monomer and its UV cured polymer (right).

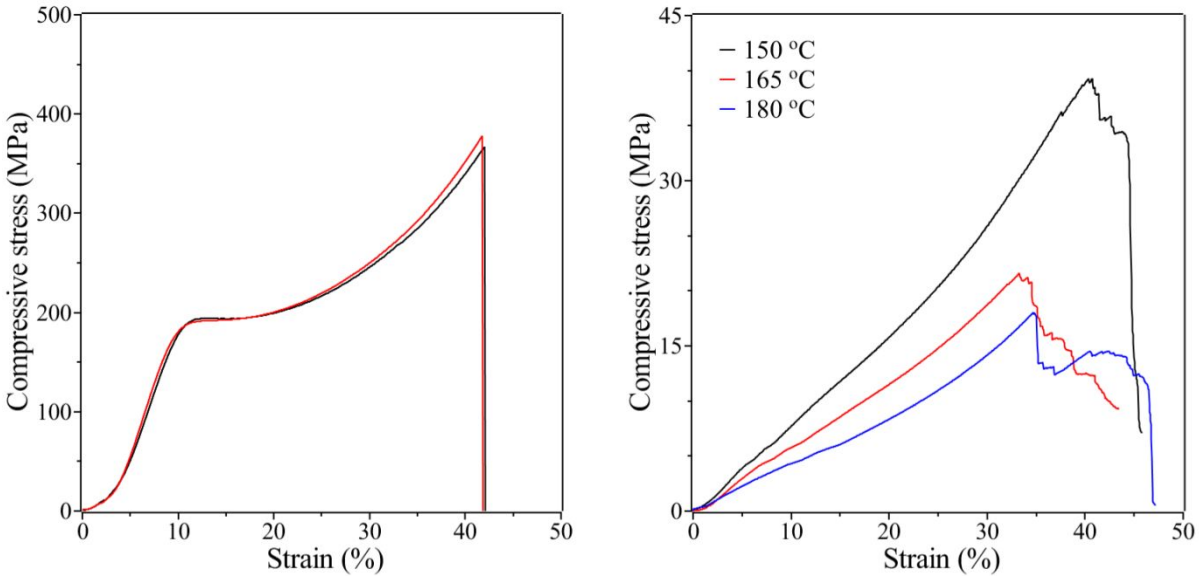

Figure S3. Compressive curves of the BPA samples at room temperature (left) and elevated temperatures (right).

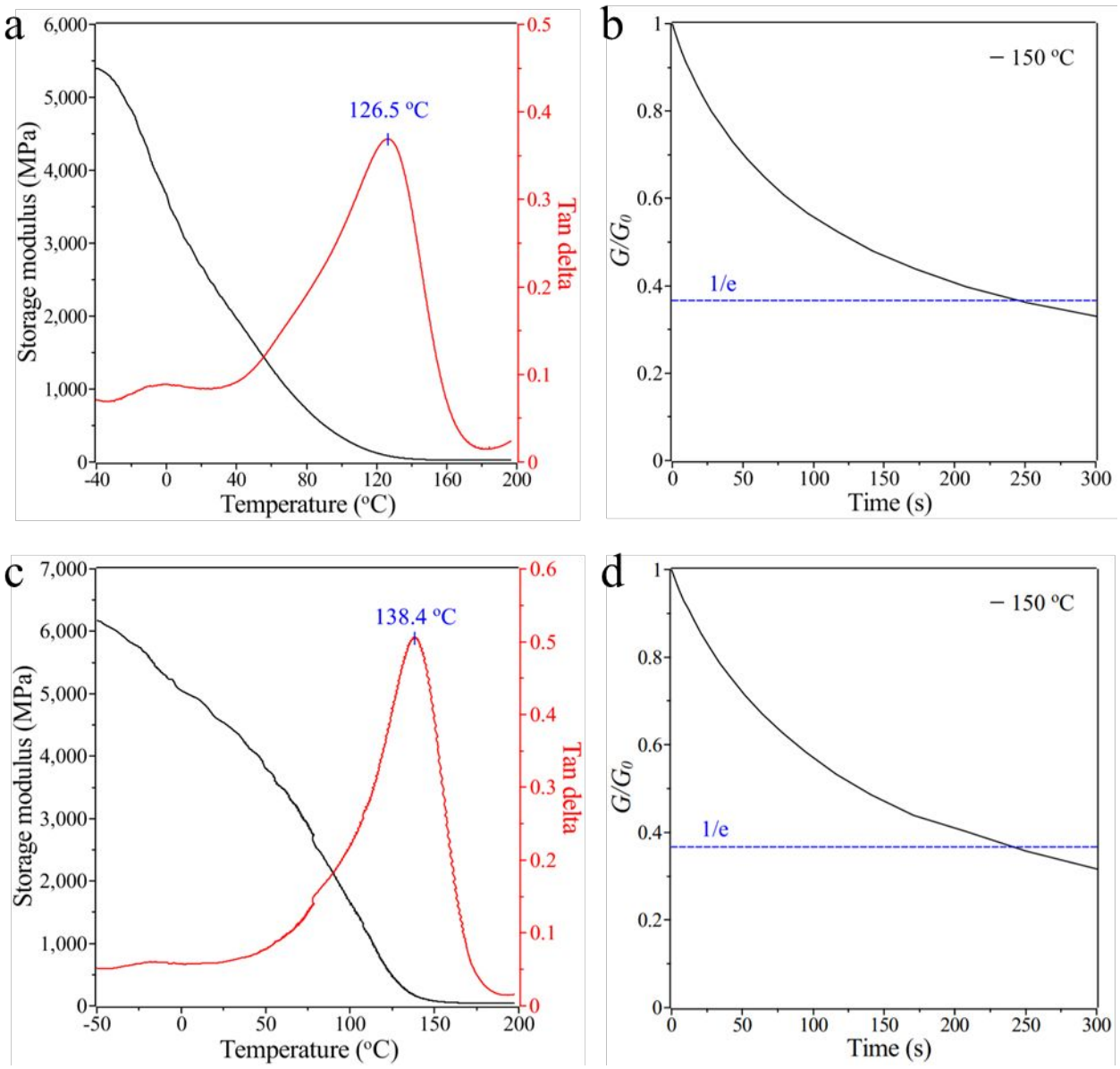

Figure S4. (a) Storage modulus and tan delta curves and (b) normalized stress relaxation curve of the BPA-BA sample at 150 °C. (c) Storage modulus and tan delta curves and (d) normalized stress relaxation curve of the BPA-MA sample at 150 °C.

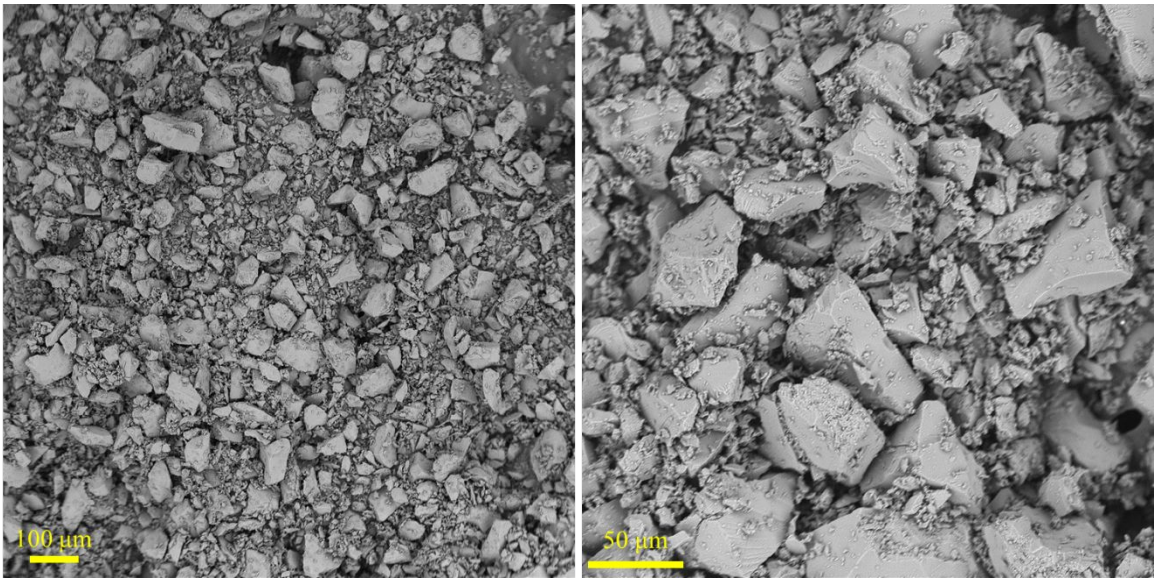

Figure S5. SEM images of the BPA thermoset polymer powders after milled at 400 rpm for 2 h at different magnifications.

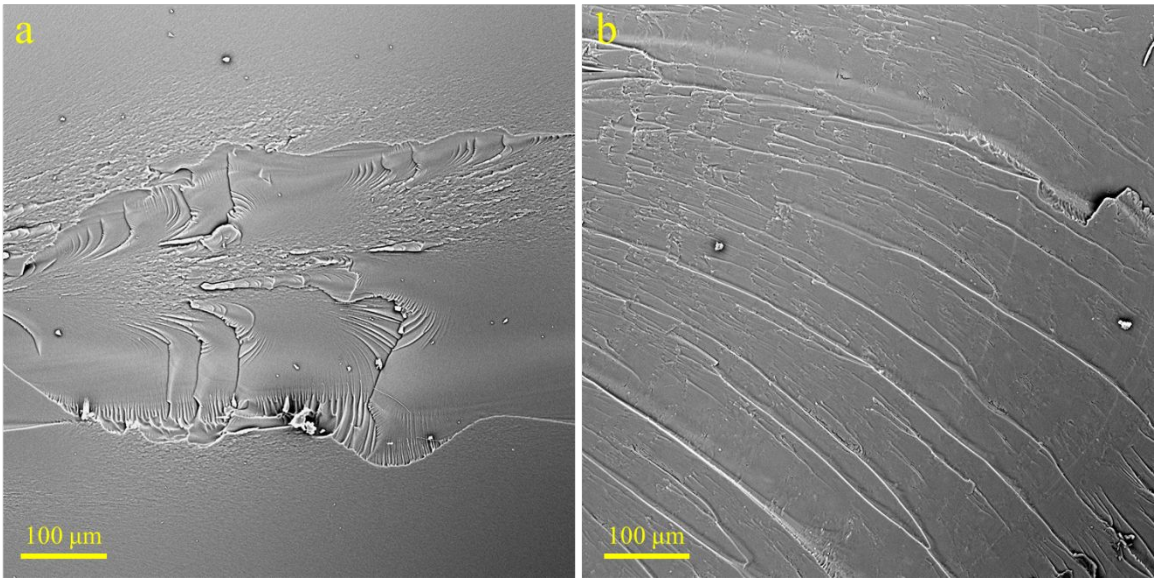

Figure S6. SEM images of the fracture surface of (a) the original BPA thermoset and (b) the recycled BPA sample after compression at 150 °C for 1 h.

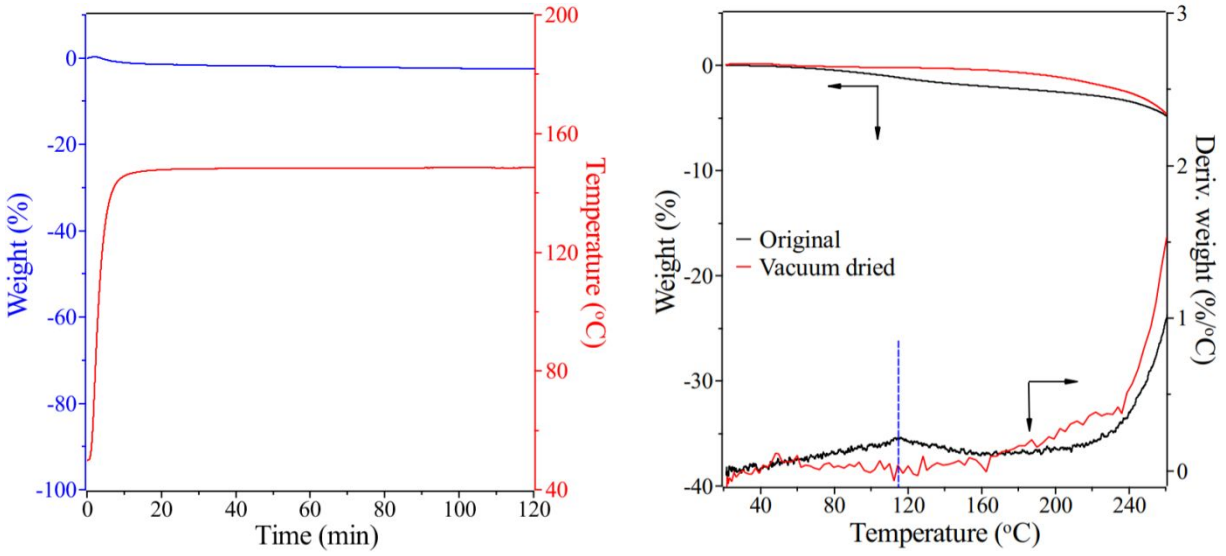

Figure S7. Isothermal degradation behavior of the BPA network at 148 °C for around 2 h (left). TG curves of as-prepared BPA network and the BPA network after vacuum drying.

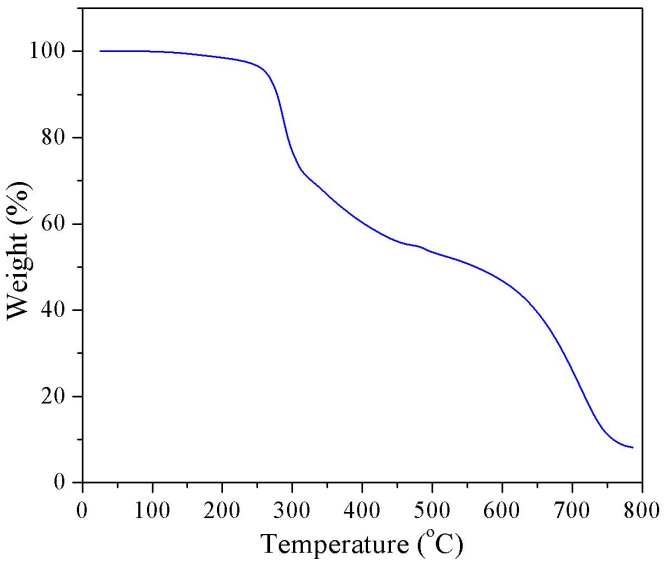

Figure S8. TG curve of the BPA sample under air atmosphere at a heating rate of 10 °C/min.

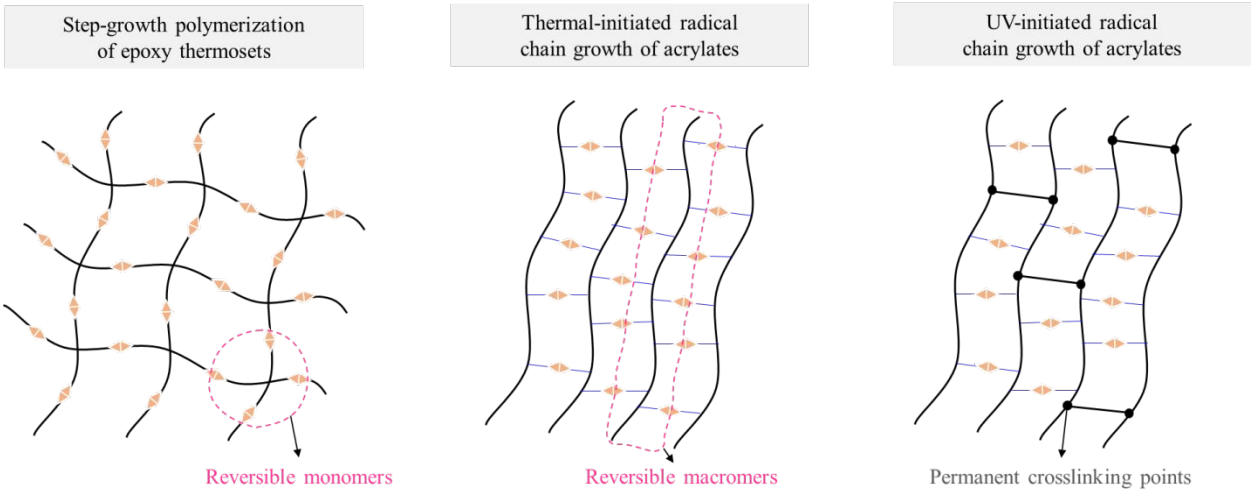

Figure S9. Three classic CANs resulting from step-growth polymerization of epoxy thermosets, thermal-initiated and UV-initiated radical chain growth polymerization of acrylates, respectively.

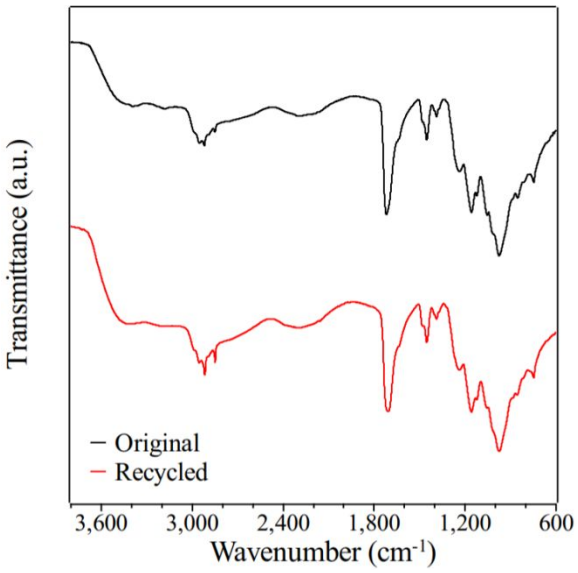

Figure S10. FTIR spectra of the original and the recycled BPA network samples.

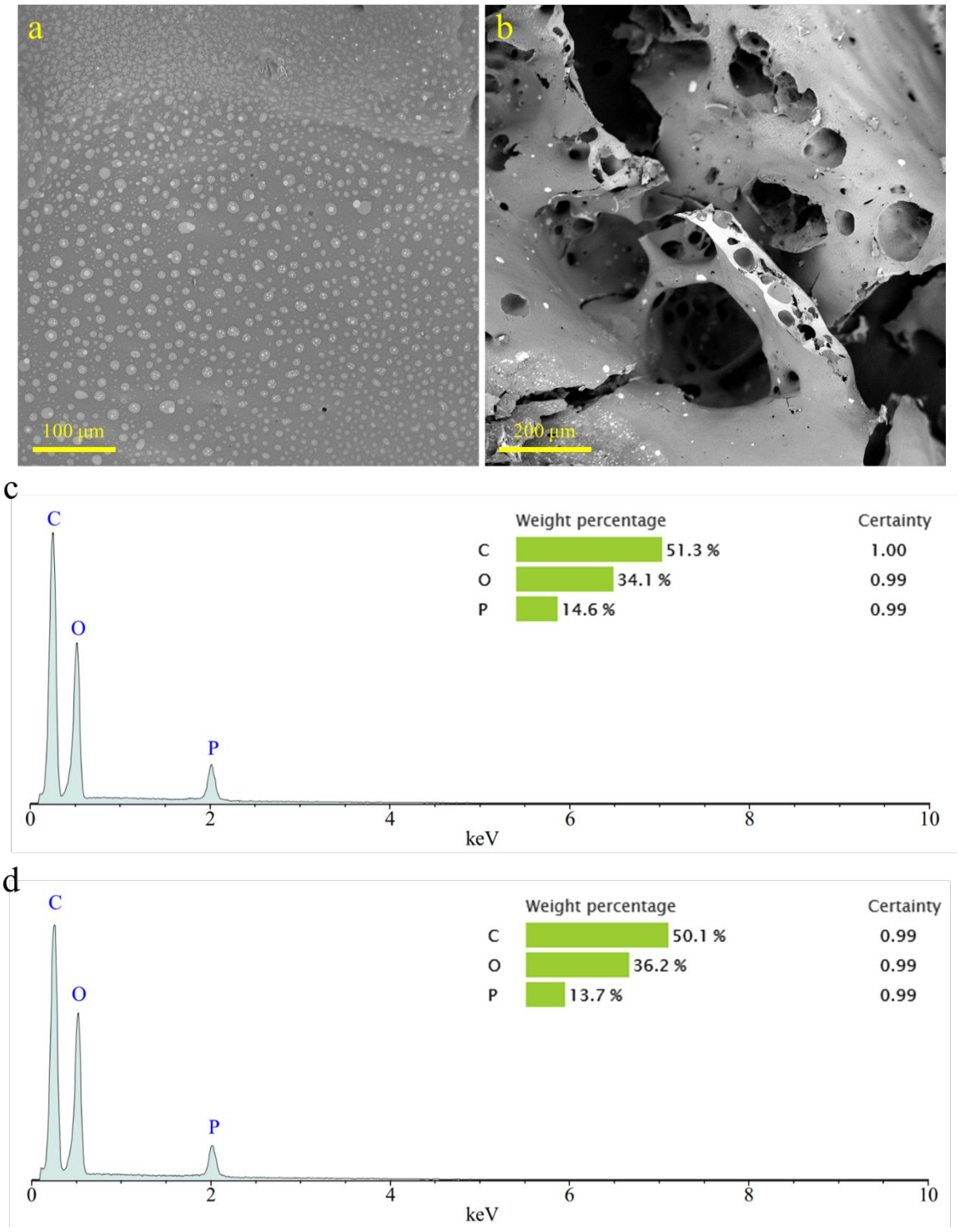

Figure S11. SEM images of (a) the surface structure and (b) innner structure of the BPA char residue. EDS results of (c) the surface structure and (d) innner structure of the BPA char residue.

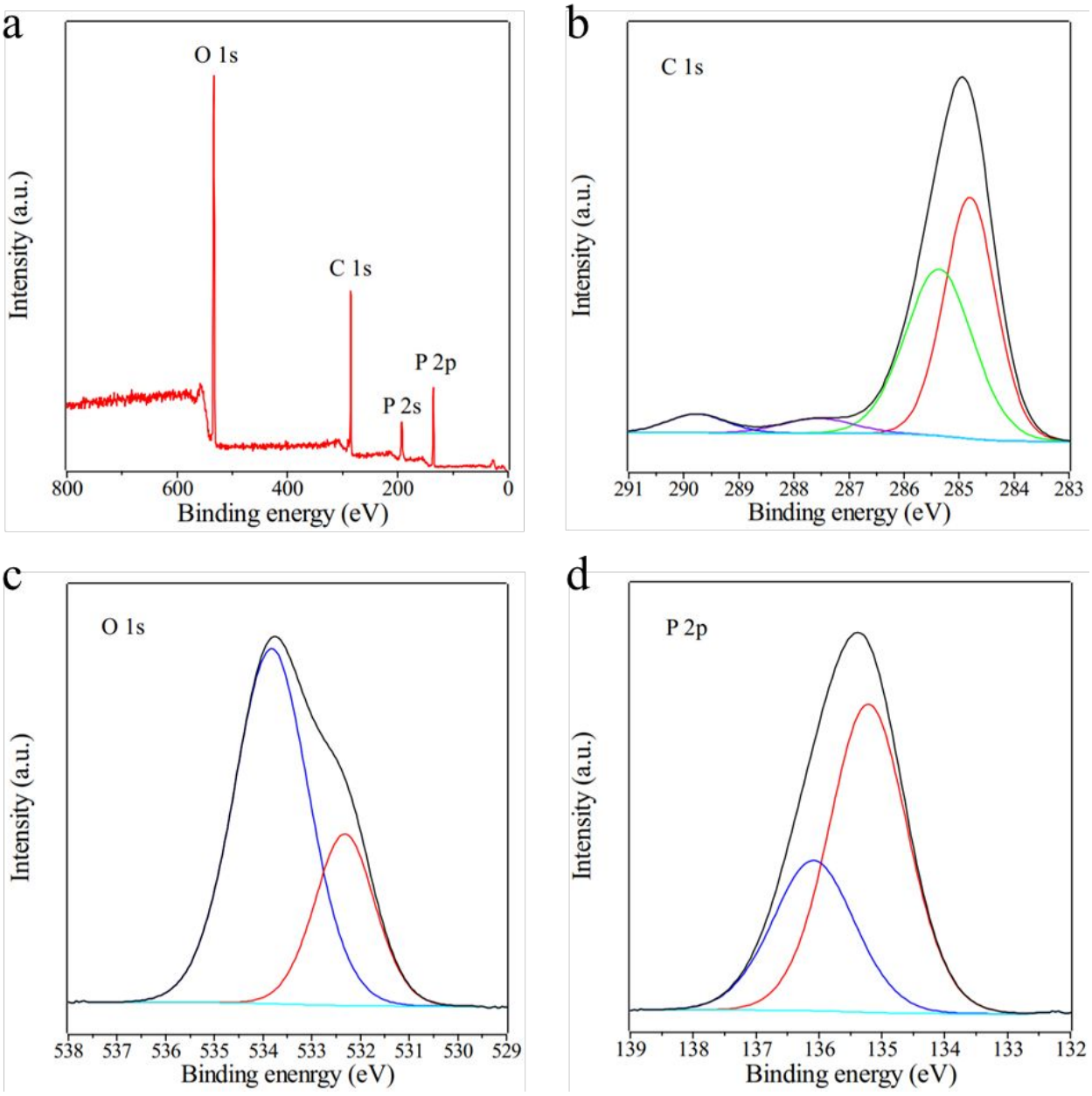

Figure S12. (a) XPS survey spectrum for the burned char of the BPA sample. High-resolution (b) C 1s, (c) O 1s, and (d) P 2p XPS spectra of the burned char of the BPA sample.

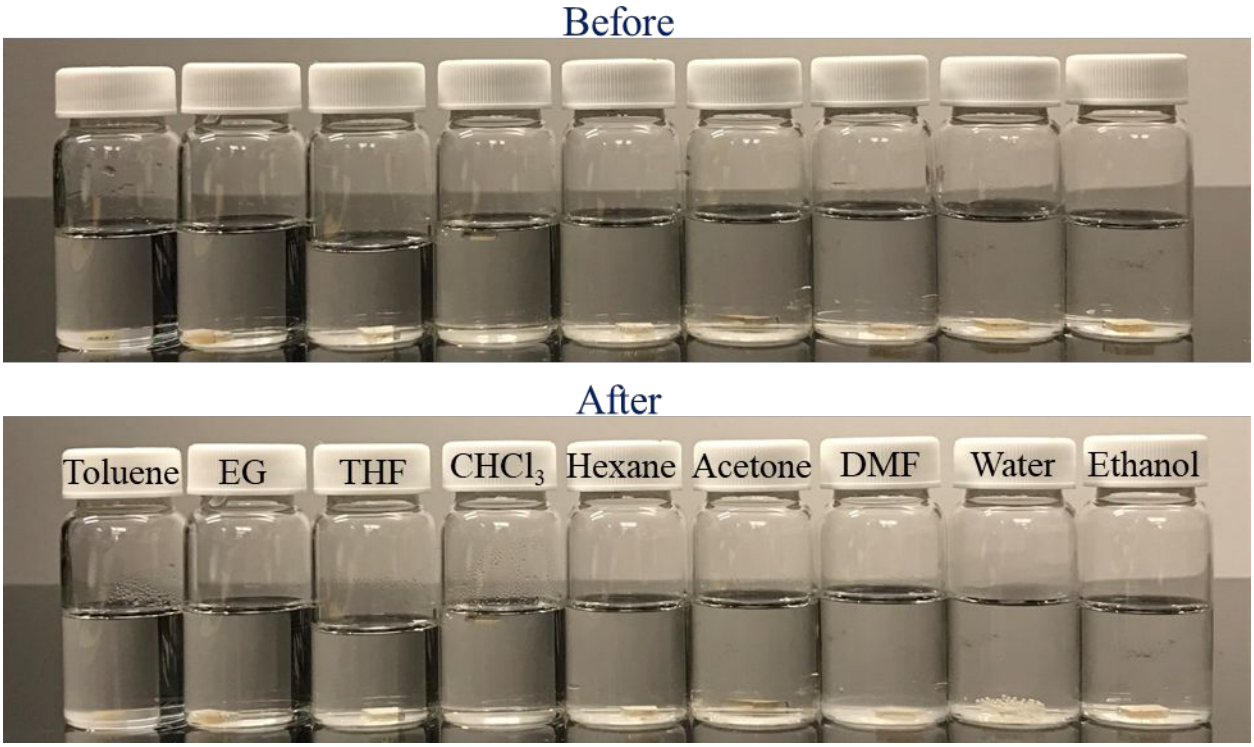

Figure S13. The dissolution experiments for the BPA network. It shows that the BPA samples were stable in the organic solvents, such as ethanol, acetone, chloroform, toluene and hexanes tetrahydrofuran (THF), ethylene glycol (EG) and dimethyl formamide (DMF) after 4 days immersion. After immersing in water for 4 days, some bubbles can be observed, indicating the possibility of hydrolyzation of the BPA networks.

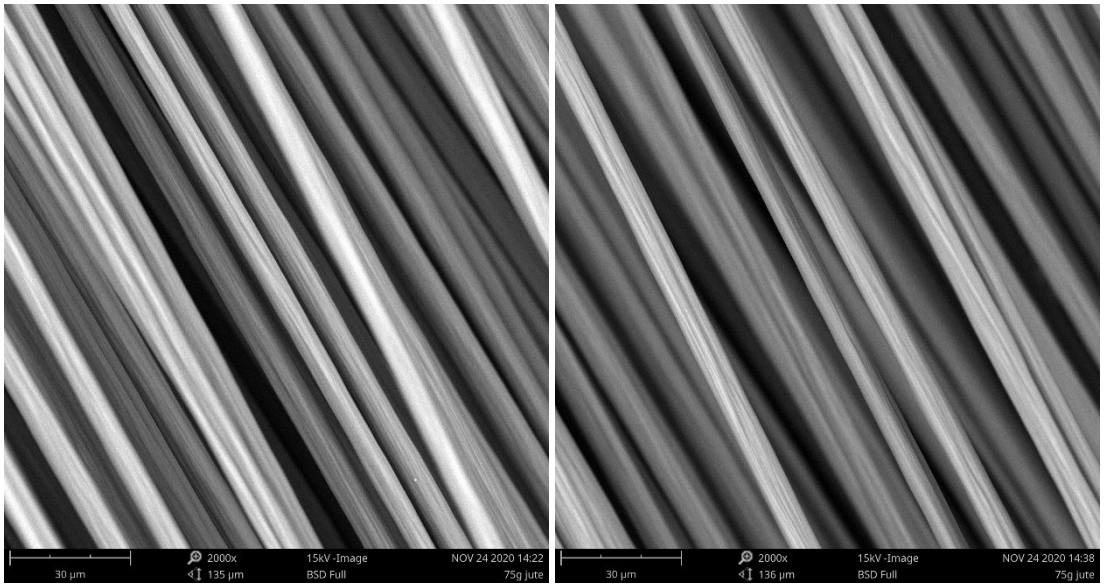

Figure S14. SEM images of the original (left) and recycled (right) carbon fibers.

Table S1. Basic properties of the BPA network.

Sample	$T_{5\%}$ (°C)	T_g (°C)	Glassy modulus (25 °C) (MPa)	Rubbery modulus (T_g + 30 °C) (MPa)	Crosslinking density (mol/m^3)
BPA	262.7	152.4	2920.6	75.7	7.1×10^3

Table S2. Summary of recycling properties of the BPA network under different conditions.

Sample	Recycling condition	Tensile strength (MPa)	Young's modulus (GPa)	Elongation at break (%)	Recycling efficiency (%)
Original	--	54.6 ± 2.0	1.5 ± 0.2	7.5 ± 1.9	--
A	50 °C, 5 h, 10 MPa	18.3 ± 4.1	1.7 ± 0.2	1.4 ± 0.1	33.5
B	125 °C, 1 h, 10 MPa	37.4 ± 0.8	1.9 ± 0.0	3.1 ± 0.1	68.5
C	150 °C, 1 h, 10 MPa	41.2 ± 3.3	2.0 ± 0.6	3.5 ± 1.6	75.5

Table S3. Comparison of recycling conditions and performances of the BPA network with those of reported dynamic networks.

System	Ref.	T_g (°C)	Recycling temperature (°C)	Δ T (°C)	Recycling time (h)	Recycling pressure (MPa)	σ_o (MPa)	σ_R (MPa)	Recycling efficiency (%)	Catalyst -free	Flame retardancy
UV cured glassy thermoset	**This work**	**152.4**	**150**	**-2.4**	**1**	**10**	**54.6**	**41.2**	**75.5**	**Yes**	**Yes**
			125	-27.4	1	10		37.4	68.5		
			50	-102.4	5	10		18.3	33.5		
	[3]	62	170	108	4	300	38.1	~31	~81.4	Yes	No
			140	78	4	300		~15	~39.4		
			80	18	4	300		~19	~49.9		
			110	48	4	300		~0.5	~1.2		
	[4]	108.3	180	71.7	2	15	44	33	75	No	No
	[5]	~55	220	165	2	500	~15.2	~13.9	~91.5	No	No
	[6]	75	150	75	2	6	36.7	14.6	40.0	Yes	No
			150	75	2	9		17.2	46.9		
			150	75	2	14		25.5	69.5		
			130	55	2	14		12.4	33.8		
			175	100	2	14		19.3	52.6		
	[7]	95	200	105	2	12	62.0	17.6	28.4	Yes	No
			150	55	2	12		13.5	21.8		
			150	55	2	9		12.7	20.5		

	[8]	113	130	80	17	-33	1	24	10	44.8	44.9	100	Yes	No
	[9]	131.1	180		48.9		2		15	117.7	96.0	81.6	Yes	No
UV cured elastomer	[10]	-116	100		216		12		22	0.23	0.21	91.3	Yes	No
	[11]	--	130		--		0.5		--	1.3	1.1	84.6	Yes	No

Δ T is the differecen between recycling temperature and glass transition temperatue;

σ_o is the tensile strength of original sample, and σ_R is the tensile strength of recycled sample;

Table S4. The atomic percentage of each elements in original and burned BPA samples tested by XPS.

Sample	P 2p	C 1s	O 1s
Original	2.54 at %	66.98 at %	30.47 at %
Burned char	17.80 at %	40.82 at %	41.39 at %

Table S5. Weight change of the BPA samples before and after organic solvents immersion for 4 days at ambient temperature.

Solvents	Before	After
Toluene	100 %	100.55 %
EG	100 %	100.19 %
THF	100 %	100.92 %
$CHCl_3$	100 %	100.42 %
Hexane	100 %	100.59 %
Acetone	100 %	100.23 %
DMF	100 %	100.62 %
Ethanol	100 %	101.02 %

Table S6. Summary of tensile properties of the original BPA composite and regenerated BPA composite.

Sample	Tensile strength (MPa)	Elongation at break (%)
Original	370.6 ± 7.9	4.1 ± 0.2
Regenerated	328.9 ± 5.2	3.6 ± 0.3

References

(1) Nishimura, Y.; Chung, J.; Muradyan, H.; Guan, Z. B. Silyl Ether as a Robust and Thermally Stable Dynamic Covalent Motif for Malleable Polymer Design. *J. Am. Chem. Soc.* **2017,** *139* (42), 14881-14884.

(2) He, C. F.; Shi, S. W.; Wang, D.; Helms, B. A.; Russell, T. P. Poly(oxime-ester) Vitrimers with Catalyst-Free Bond Exchange. *J. Am. Chem. Soc.* **2019,** *141* (35), 13753-13757.

(3) Li, C.; Liu, J. W.; Chen, Y. Z.; Li, T.; Cai, X. X.; Sung, J. G.; Sun, X. Z. S. S. Hybrid Network via Instantaneous Photoradiation: High Efficient Design of 100% Bio-Based Thermosets with Remoldable and Recyclable Capabilities after UV Curing. *Chem. Eng. J.* **2018,** *336*, 54-63.

(4) Wang, S. P.; Wu, Y. G.; Dai, J. Y.; Teng, N.; Peng, Y. Y.; Cao, L. J.; Liu, X. Q. Making Organic Coatings Greener: Renewable Resource, Solvent-Free Synthesis, UV Curing and Repairability. *Eur. Polym. J.* **2020,** *123*, article no. 109439.

(5) Zhang, B.; Kowsari, K.; Serjouei, A.; Dunn, M. L.; Ge, Q. Reprocessable Thermosets for Sustainable Three-Dimensional Printing. *Nat. Commun.* **2018,** *9*, article no. 1831.

(6) Li, A.; Fan, J. Z.; Li, G. Q. Recyclable Thermoset Shape Memory Polymers with High Stress and Energy Output via Facile UV-Curing. *J. Mater. Chem. A* **2018,** *6* (24), 11479-11487.

(7) Li, A.; Challapalli, A.; Li, G. Q. 4D Printing of Recyclable Lightweight Architectures Using High Recovery Stress Shape Memory Polymer. *Sci. Rep.* **2019,** *9*, article no. 7621.

(8) Li, X. P.; Yu, R.; He, Y. Y.; Zhang, Y.; Yang, X.; Zhao, X. J.; Huang, W. Four-Dimensional Printing of Shape Memory Polyurethanes with High Strength and Recyclability Based on Diels-Alder Chemistry. *Polymer* **2020,** *200*, article no. 122532.

(9) Wang, S. P.; Teng, N.; Dai, J. Y.; Liu, J. K.; Cao, L. J.; Zhao, W. W.; Liu, X. Q. Taking Advantages of Intramolecular Hydrogen Bonding to Prepare Mechanically Robust and Catalyst-Free Vitrimer. *Polymer* **2020,** *210*, article no. 123004.

(10) Liu, Z.; Hong, P.; Huang, Z. Y.; Zhang, T.; Xu, R. J.; Chen, L. J.; Xiang, H. P.; Liu, X. X. Self-Healing, Reprocessing and 3D Printing of Transparent and Hydrolysis-Resistant Silicone Elastomers. *Chem. Eng. J.* **2020,** *387*, article no. 124412.

(11) Aizpurua, J.; Martin, L.; Fernandez, M.; Gonzalez, A.; Irusta, L. Recyclable, Remendable and Healing Polyurethane/Acrylic Coatings from UV Curable Waterborne Dispersions Containing Diels-Alder Moieties. *Prog. Org. Coat.* **2020,** *139*, article no. 105460.